Hindawi
Shock and Vibration
Volume 2022, Article ID 6460090, 12 pages
https://doi.org/10.1155/2022/6460090

Research Article

Research on Mechanical Properties and Macroscopic Fracture Evolution of Rock with Different Joint Plane Features

Yongjiang Yu,[1] **Jingjing Liu**,[1] **Pengbo Wang**,[2] **Yuntao Yang**,[1] **and Shangqing Zhao**[1]

[1]*College of Mining Engineering, Liaoning Technical University, Fuxin 123000, China*
[2]*Gas Research Branch, China Coal Technology and Engineering Group Chongqing Research Institute, Chongqing 400037, China*

Correspondence should be addressed to Jingjing Liu; ljjyx8341@163.com

Received 10 June 2022; Revised 10 August 2022; Accepted 25 August 2022; Published 20 September 2022

Academic Editor: Yonggang Zhang

To analyze the safety of geological engineering, experimental research on the mechanical properties of the rock joint plane is critical. In this paper, triaxial compression tests are carried out on rock specimens with the different prefabricated joint planes, including different dip angles, roughness, confining pressure and surrounding rock strength, and the strength characteristics, failure modes, stress evolution laws, and crack propagation laws are revealed. The test results show that when the specimen is damaged, the strain, peak stress, and residual strength all increase with the increase of roughness, confining pressure, and strength of surrounding rock but decrease significantly with the increase of joint plane angle. With the increase of stress, the stress-strain curve shows multiple fluctuations, indicating that the specimen occurs multiple slip-stable phenomena during the loading process. With the increase of the angle, the multiple cracks of the specimen gradually merge, and the cracks are always vertical to the joint plane, showing splitting failure. As the roughness of the joint plane increases, the possibility of the joint plane sliding becomes smaller, and the splitting mode of the specimen develops from multiple fractures to a single fracture. As the strength of the surrounding rock increases, the slope of the stress-strain curve gradually increases, and the splitting mode develops from a small number of single splits to multiple splitting penetration failures. The increase of the confining pressure significantly improves the failure strength of the specimen, and the crack number of the damaged specimen also increases significantly. The research results provide theoretical support for scientific analysis of the stability of underground engineering under the disturbance of fissures or faults.

1. Introduction

The natural rock mass usually refers to the rock that is in a specific state of stress in the engineering construction and geological disasters, and it is cut by various joint planes; these joint planes are relatively weak in mechanical strength, which leads to the discontinuity, inhomogeneity, and anisotropy of the mechanical properties of the rock mass. The structural characteristics of rock mass play an important role in controlling the deformation failure mode and strength characteristics of rock mass under certain load conditions. Due to the limited test condition and cost, it is often difficult to carry out field tests of rock masses with joint planes. At the same time, the sampling of natural joint plane rock mass is difficult in the indoor test, and even if the sampling is sufficient, its dispersion is very large, which is difficult to meet the needs of experimental design. Therefore, it is particularly important to select rock samples with prefabricated joint planes or artificial joint planes for relevant tests. Many related experimental studies have been carried out by predecessors.

Yang et al. believed that roughness is one of the important factors affecting the strength and deformation characteristics of the jointed rock mass; they used the GCTS high-temperature and high-pressure dynamic-static rock triaxial test system to carry out the triaxial compression test on the rock samples with different joint roughness and analyzed the corresponding acoustic emission characteristics. It is found that the joint plane directly leads to a significant decrease in the strength of the jointed rock, and with

the increase of the JRC value, the shear strength of the rock joint plane increases, and the triaxial compressive strength of the rock sample also increases. The fragile failure is transformed into ductile failure [1]. Dong and Tian used the THMC multifunctional coupling testing machine to conduct uniaxial compression and conventional triaxial compression tests to study the mechanical properties and failure mechanism of marble under external loads. It was found that the plastic deformation of marble increases with the confining pressure, and the failure of rock samples is achieved by increasing the internal friction angle φ and decreasing the cohesion C [2]. Nasseri et al. analyzed the failure modes of four kinds of anisotropic schists from the macro and micro scales and found that the variation range of principal stress direction (σ_1) in different directions (β) is from 0° to 90° when samples are in unconfined and confined states ($\sigma_3 = 100$ MPa) [3]. Similarly, through triaxial compression tests, including unloading cycles, Niandou et al. studied the anisotropic elastic response, plastic deformation, and failure behavior of shale, and it was found that the failure behavior of shale was anisotropic and largely depended on the confining pressure and loading direction [4]. Regarding the influence of joint plane angle on failure mode and strength of rock, Mao and Yang used the single weak plane theory to study the change of the compressive strength of slate rock mass with a single group of structural planes with the joint plane orientation and found that when the joint plane angle was about 51.7°, the compressive strength of slate reaches the minimum value; and with the change of the joint plane, three failure modes can be generated, including slip failure along the joint plane, shear failure, and composite failure [5]. Based on the Coulomb strength criterion, Han et al. established a mathematical model under the σ_1–σ_3 coordinate system and used the positional relationship between the fracture plane and the rock mass strength curve to study the strength and failure mode of the rock mass passing through the fracture and discussed the relationship between the strength of rock mass with the penetrating fracture with angle, cohesion, internal friction angle, block cohesion, and internal friction angle of the fracture surface, obtaining relevant criteria for the failure mode of penetrating fractured rock mass [6]. Through a series of experiments, Li et al. studied the stress-strain relationship of rock mass under loading and unloading conditions and concluded the anisotropy, size effect, and rheological properties of the unloaded rock mass. It was found that the influence of different joint plane directions on the unloading rock mass is obvious; with the increase in joint plane size, the tensile strength, compressive strength, deformation modulus, Poisson's ratio, and anisotropy of rock mass all decrease. The rheological properties of the rock are closely related to the tensile stress, and the rheological rate varies with the axial stress and confining pressure [7]. By conducting a series of static triaxial tests on artificial cylindrical specimens that simulated jointed rock mass with different dip angles, Liu et al. understand the deformation and failure laws of rock mass with penetrating joints, obtained the relevant stress-strain curves and failure characteristics, and then analyzed the influence of joint plane angle on the mechanical properties of jointed rock samples [8]. Considering that effectively modeling the effect of rock joints on rock mass behavior may be beneficial in rock engineering, Zheng et al. found that the angle of the joint plane has a great influence on the mechanical properties of the rock samples; moreover, they prepared rock samples with structural plane angles of 15°, 30°, 45°, and 60° to carry out uniaxial compression tests and triaxial compression tests with confining pressures of 100 KPa, 200 KPa, and 300 KPa; thus, the effect of joint plane angle on mechanical and deformation properties of rock samples was explored [9]. Based on the 1.0 Hz frequency cyclic triaxial test results, Liu and Liu analyzed the mechanical behavior of artificial jointed rock samples with different joint angles under different stress amplitudes and confining pressures. It was found that the dynamic strength decreases with the increase of the joint angle and increases with the increase of the confining pressure. The stress ratio (the ratio of the maximum stress under cyclic loading to the static triaxial compressive strength) can comprehensively reflect the effects of joint angle, confining pressure, and stress amplitude [10]. Mahboubi and Ajorloo present the experimental parametric study of the mechanical response of various plastic concretes in unconfined and triaxial compression tests and studied the effect of specimen curing age, cement factors, bentonite content, and confining pressure on shear strength and permeability of plastic concrete [11]. Under the condition of different ages, different mix ratios, and different confining pressure, Pashang Pisheh and Mir Mohammad Hosseini carried out triaxial compression tests and studied the stress-strain behavior of the material and the changes in its strength parameters. It is concluded that increasing the confining pressure can make the properties of the material similar to those of stronger ductile materials, and the compressive strength is also significantly improved [12]. Donath elucidated that plane anisotropy has a significant effect on both fracture strength and shear fracture angle of rocks [13]. By extending the McClintock–Walsh correction method of Griffith's theory to brittle fractures in anisotropic rocks, Walsh and Brace proposed that anisotropy is mainly due to the preferential orientation of cracks in rocks, and the ideal mathematical model for fracture analysis is the elastic isotropic medium that includes nonrandom fractures for Griffith crack arrays [14]. In order to study the strength and deformation properties of jointed rock mass under a true triaxial stress state, Reik and Zacas performed an indoor triaxial compression test on an ideal model of the jointed rock mass to investigate the influence of different joint shapes and horizontal stress ratios on the mechanical behavior of jointed rocks [15]. Based on the current rock mechanics test method, He et al. established a numerical model of the triaxial compression test and identified the feasibility of the model. Taking the Fengtan Hydropower Station as the background, the numerical simulation of the triaxial compression test of the rock mass with the joint plane was carried out, and the size effect of the anisotropy of the equivalent elastic modulus of the rock mass and the influence of the dip and spacing of the joint plane of the rock mass on the equivalent elastic modulus of the rock mass were investigated [16]. Nishiyama

et al. used fluorescence technology to study the behavior of granite from the prefailure stage to the postfailure stage in the triaxial compression test from a geological point of view and observed the microscopic changes of the specimen in the failure process of different stages [17]. Arzúa et al. performed a series of compression tests on artificially jointed granite specimens with two joint groups in a fully servo-controlled press and studied the full stress-strain response of these specimens [18]. Lagioia and Nova conducted experimental and theoretical studies on the behavior of calcareous rocks under different axisymmetric loading. They used the strain hardening plastic theory to establish the mathematical model and describe the overall properties of limestone in different types of triaxial compression tests [19]. Serdengecti and Boozer present the results of dynamic triaxial compression tests to characterize the strength of sandstone, limestone, and gabbro under controlled stress, strain rate, and temperature conditions and propose the mechanical state of the Fusanghofen limestone Equation [20]. Considering that rock mass is often subjected to cyclic loads in engineering practice, the mechanical properties of the rock are significantly different from those under conventional loading conditions. The mechanical behavior and fatigue of intact rocks have been extensively studied. However, the mechanical fatigue properties of rock masses with surface cracks and their damage evolution models are not well understood. Lin et al. considered five preexisting surface crack angles (0°, 15°, 30°, 45°, and 60°) and three different maximum cyclic stress levels (19.1 MPa, 25.6 MPa, and 30.3 MPa) to perform a series of fatigue damage tests on yellow sandstone specimens. Based on the increased strain energy, the effect of macroscopic cracks on rock damage is studied, and a constitutive model of fatigue tests is established based on the coupled macroscopic and microscopic damage. The research results have certain reference values for the long-term stability evaluation of fractured rock mass engineering [21]. Zhou et al. studied the applicability of the equivalent rock mass (ERM) technique based on the particle method. They found that deformation and failure were affected by joint degradation, formation of microcracks in intact rock, interaction between two joints, and interaction between microcracks and joints [22]. The strength and deformability of rock masses crossed by nonpersistent joints are governed by the complex interaction of joints and intact rock bridges. The numerical simulations of synthetic rock mass (SRM) provide a promising method for rock mass analysis, but it is not compared with actual physical experiments. By using the discrete element software PFC3D to model the SRM, Bahaaddini et al. studied the influence of the geometric parameters of the joints on the failure mechanism, unconfined compressive strength, and deformation modulus of the rock mass. It was found that the failure mode was mainly determined by the joints direction and the step angle, and compared to the principal stress direction, the joint direction relative is the parameter that most affects the rock mass properties [23].

The above research mainly focuses on the influence of single factors such as confining pressure, surrounding rock strength, roughness, or dip angle of joint plane on the mechanical properties of rock mass but ignores their coupling effect on joint rocks. In this paper, the influence of the angle, roughness, confining pressure, and lithology (surrounding rock strength) of the joint plane on the rock mass strength, failure form, and macroscopic fracture evolution law is comprehensively considered. The self-developed visual coal-rock fluid-solid coupling test is used to conduct triaxial compression tests on four groups of specimens with different angles, roughness, confining pressure, and lithology. The research results provide a useful reference for revealing the stability of underground engineering under the disturbance of cracks or faults by studying the mechanical tests of rock specimens with different joint plane characteristic parameters.

2. Mudstone Creep Disturbance Test Scheme

2.1. Test Equipment. As shown in Figure 1, the visuable coal-rock fluid-solid coupling test system was adopted in this test, and it is independently developed by the Mechanics Laboratory of Liaoning University of Engineering and Technology. The allowed maximum static load of the system is 300 kN, and the confining pressure is applied to the specimen by filling nitrogen into the closed pressure chamber.

2.2. Specimen Preparation. The roof rock mass at 200 m from the material path 7303 in mining area III5 of Kongzhuang Coal Mine was collected, and it was made into specimens of mudstone, fine sandstone, and coarse sandstone in accordance with the Chinese Standard for Test Methods of Engineering Rock Mass (GB/T 50266-99). The processed specimens were cut into rock masses with different angles according to the design plan, and the 10-, 30-, and 60-mesh screens were used to divide them into three groups: coarse sand, medium sand, and fine sand. The sample and the sieved sand are shown in Figure 2.

The infiltrated yellow mud was covered on the joint plane on both sides of the specimen to bond sand; thus, the roughness of the joint plane can be simulated. Then, the two plates of the test specimen were bonded and placed in the laboratory until the yellow mud dried to reach a certain strength, as shown in Figure 3 [24].

2.3. Test Scheme. The test was uniformly controlled by force loading, and the loading rate was 200 N/s. The comparison tests were performed from four aspects, including joint angle, confining pressure, joint plane roughness, and surrounding rock strength (lithology). The specific schemes are as follows.

2.3.1. Only the Joint Angle Is Different. The same amount of yellow mud was used to stick equal weight of medium sand as the filling surface of mudstone specimens, and the joint angle was set to be 10°, 15°, 20°, 25°, 30°, 35°, and 40° when the roughness of the structural surface was kept the same. Specimens were subjected to triaxial compression tests.

(a) (b)

Figure 1: Visuable coal-rock fluid-solid coupling test system: (a) measurement and control system and (b) loading device.

Figure 2: Specimen and sand with different particle sizes.

2.3.2. Only the Roughness of the Joint Plane Is Different. The fine sandstone specimen with the joint angle of 25° was selected, and the sand with different particle sizes was adhered to with the same amount of yellow mud as the filling surface to model the different roughness of the structural surface. The triaxial compression test under the confining pressure of 1 MPa was performed.

2.3.3. Only the Strength of the Surrounding Rock Is Different. The fine sandstone and coarse sandstone specimens with a joint plane angle of 25° were selected, respectively, and medium sand was added to the filling surface. The triaxial compression test under the confining pressure of 1 MPa was performed.

2.3.4. Only the Confining Pressure Is Different. The fine sandstone specimen with the joint plane angle of 25° was selected, and the fine sand was added to the filling surface. The triaxial compression tests under the confining pressure of 1 MPa, 2 MPa, and 3 MPa were performed.

3. Analysis of the Results

3.1. Stress and Crack Evolution of Different Discontinuities. The test results of the first scheme are shown in Figure 4. It can be seen that the angle of the joint plane has a certain influence on the mudstone. When the angle of the joint plane is 10°, the deviatoric stress curve of the mudstone specimen is linear and grows very fast before failure, the peak stress reaches 27.25 MPa, and the specimen does not occur significant slipping during loading move traces. When the angle of the joint plane is 15° and 20°, the stress-strain curve has a similar trend, and the peak stress is 19.2 MPa and 16.8 MPa, respectively. With the increase of the angle of the joint plane, the failure peak stress of the specimen decreases significantly. When the joint plane angles are 25°, 30°, 35°, and 40°, the peak strengths are 14 MPa, 11.2 MPa, 9.8 MPa, and 7.6 MPa, respectively. With the continuous increase of the stress, the stress-strain curve shows multiple fluctuated rising, indicating that the specimen has multiple slip-stable phenomena during the loading. When the angle of the joint plane is 40°, the specimen undergoes severe slip instability,

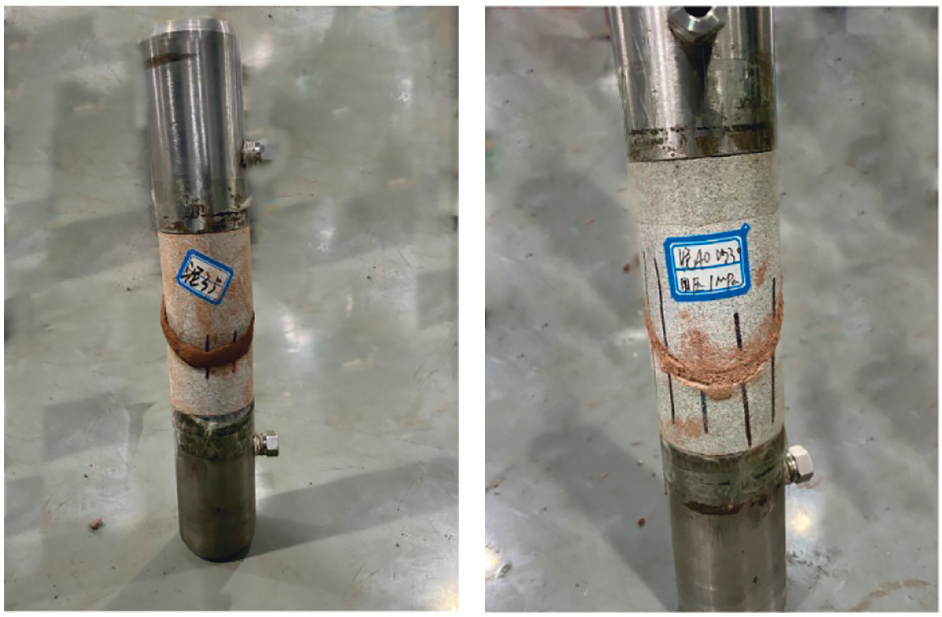

(a) (b)

Figure 3: Test specimens.

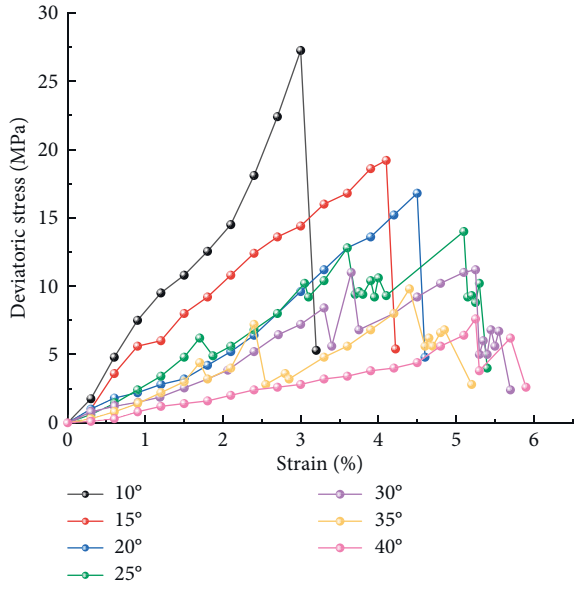

Figure 4: Stress evolution of mudstone specimens with different joint plane angles.

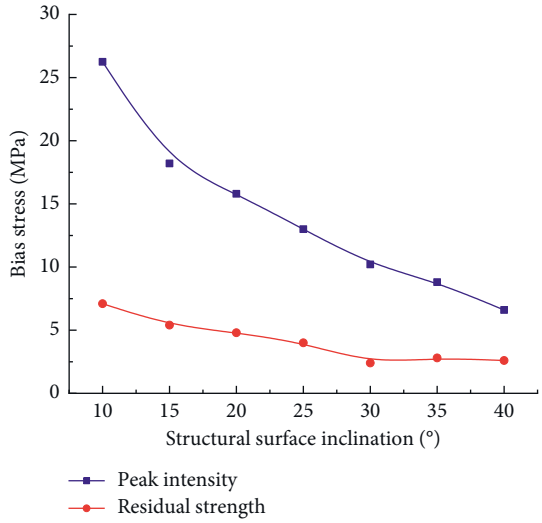

Figure 5: Variation curve of peak strength and residual strength of specimen with joint plane angle.

and its strength is significantly reduced. To sum up, when the angle of the joint plane is small, the strength of the mudstone specimen is higher; the stress growth rate is faster; and the instability failure is not easy to occur. As the angle of the joint plane increases, the peak strength of the mudstone decreases, and when this angle exceeds 25°, the mudstone specimen will experience multiple unstable slips; the two disks will eventually slip along the joint plane; and the buckling failure will occur before reaching its ultimate strength.

In order to systematically study the influence of the angle of the joint plane on the mechanical properties of mudstone specimens, the peak strength, residual strength, and elastic modulus were obtained according to the stress-strain curve. The peak strength characterizes the bearing capacity of the rock sample and has a very important influence on the stability of the rock and the safety of the structure. Figure 5 shows the variation curve of the peak strength and residual strength of the specimen with the angle of the joint plane. With the increase of the angle of the joint plane, the peak strength and residual strength of the specimen both show a downward trend, and the decreasing amplitude of peak strength is much more than the residual strength. Therefore, the elastic modulus of the specimen is used to describe the influence of different joint plane angles on the strength of the specimen.

Table 1: Triaxial compression test results of mudstone specimens with different joint plane angles.

α/°	Failure stress (MPa)		Elasticity modulus (GPa)
	σ_3	σ_1	
10°	1	27.25	9.58
15°	1	19.2	7.67
20°	1	16.8	2.8
25°	1	14	3.0
30°	1	11.2	1.79
35°	1	9.8	1.83
40°	1	7.6	1.17

Figure 6: Fragmentation characteristics of mudstone specimens with different joint plane angles: (a) standard mudstone specimen, (b) joint plane angle of 15°, (c) joint plane angle of 20°, (d) joint plane angle of 25°, (e) joint plane angle of 35°, and (f) joint plane angle of 40°.

The variation of the elastic modulus with the angle of the joint plane is shown in Table 1. It can be seen that when the angle of the joint plane is at a low level, the elastic modulus of the specimen decreases sharply with the increase of the angle of the joint plane. When the angle of the joint plane is greater than 20°, the elastic modulus of the specimen decreases gradually. The stiffness of the specimen tends to be stable when the angle of the joint plane increases to a certain extent.

In order to understand the fracture characteristics and crack evolution law of mudstone specimens with different joint plane angles, some failed specimens with obvious failure characteristics are selected and shown in Figure 6. It can be seen that the fracture characteristic of the intact standard mudstone specimen shows an obvious X-shaped conjugate inclined plane shear failure. With the increase of the joint plane angle, the crack generated in the specimen gradually transforms from multiple (Figures 6(b) and 6(c)) to single (Figures 6(e) and 6(f)), and the cracks are always perpendicular to the joint plane and show splitting failure. With the increase of the joint plane angle, the specimen occurs more obvious slip along the joint plane, which means the number of splitting fissures of the failed specimen decreases, the relative slippage of the two disks of the specimen increases, and the possibility of slippage on both sides of the specimen increases significantly. When this angle is 0°, the failure type of the specimen is shear failure; when this angle is small, the failure type is splitting failure; when this angle is large, slip instability occurs along the joint plane.

Combining Figures 4 and 6, it can be known that the increase of the joint plane angle significantly reduces the strength of the specimen, causing an obvious slip-stabilization phenomenon during the failure process of the specimen. Besides, as this angle increases, the number of splitting fissures gradually decreases, and the relative slip of the two disks of the specimen increases, making the possibility of slippage on both sides of the specimen increases significantly. When this angle is equal to 0, the failure type of the specimen is a shear failure; when this angle is relatively small, the failure type is splitting failure; when this angle is relatively large, slip instability occurs along the structural plane.

3.2. Stress and Crack Evolution of Different Roughness of Discontinuities. The test results of the second scheme are shown in Figure 7. It can be seen that the greater the roughness of the joint plane, the greater the stress peak value at failure. This is because the roughness increases the friction coefficient between the two disks and the joint plane, and the overall stress strength of the fine sandstone is improved. During the loading process, the interface effect of the structural surface is obvious. Before the specimen is damaged, there are many obvious errors between the specimen and the structural surface, that is, the process of sliding-stable-sliding, and the corresponding stress curve shows a wavy shape. The concave stage in the stress-strain curve reflects the compaction stage of the specimen, in which the specimen is obviously dislocated. With the load increase, the two-disk specimen is relatively stable, and the initial sliding can be regarded as the compaction of the filler and the initial slip stage of the structural surface; the middle and late stages of slipping can be understood as the slip stage of the structural surface. In summary, the greater the roughness of the structural surface, the greater the friction coefficient, the greater the bearing stress of the specimen, and the less the possibility of the structural surface sliding.

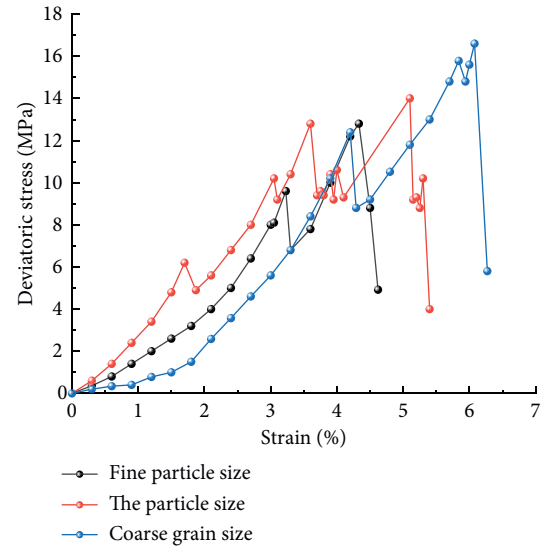

Figure 7: Stress evolution of mudstone specimens with different joint plane roughness.

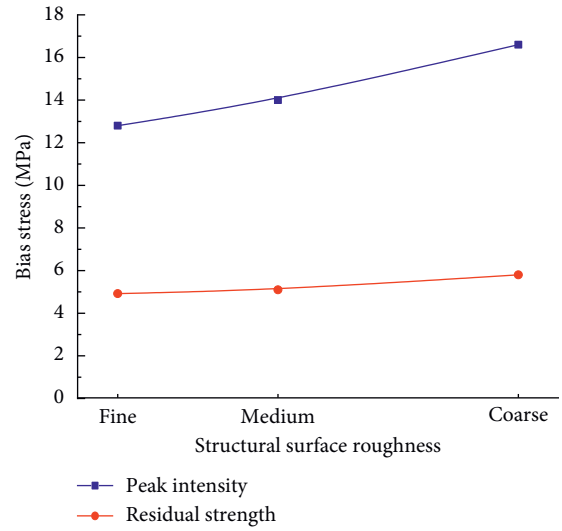

Figure 8: Variation curve of peak strength and residual strength of specimen with surface roughness.

In order to systematically study the influence of joint plane roughness on the mechanical properties of fine sandstone specimens, the peak strength, residual strength, and elastic modulus were according to the stress-strain curve, as shown in Figure 8 and Table 2.

It can be known from Figure 8 and Table 2 that with the increase of the structural surface roughness, the peak strength and residual strength of the specimen both show an upward trend, and the increased amplitude of the peak strength is much higher than that of the residual strength. The elastic modulus of the specimen increases first and then decreases with the roughness of the joint plane and is the smallest for coarse sand. The stiffness of the specimen tends to be stable when the roughness of the structural surface increases to a certain extent.

Table 2: Triaxial compression test results of fine sandstone specimens with different roughness.

Roughness	Failure stress (MPa)		Elasticity modulus (GPa)
	σ_3	σ_1	
Fine particle size	1	12.8	4.32
Particle size	1	14	4.49
Coarse grain size	1	16.6	3.98

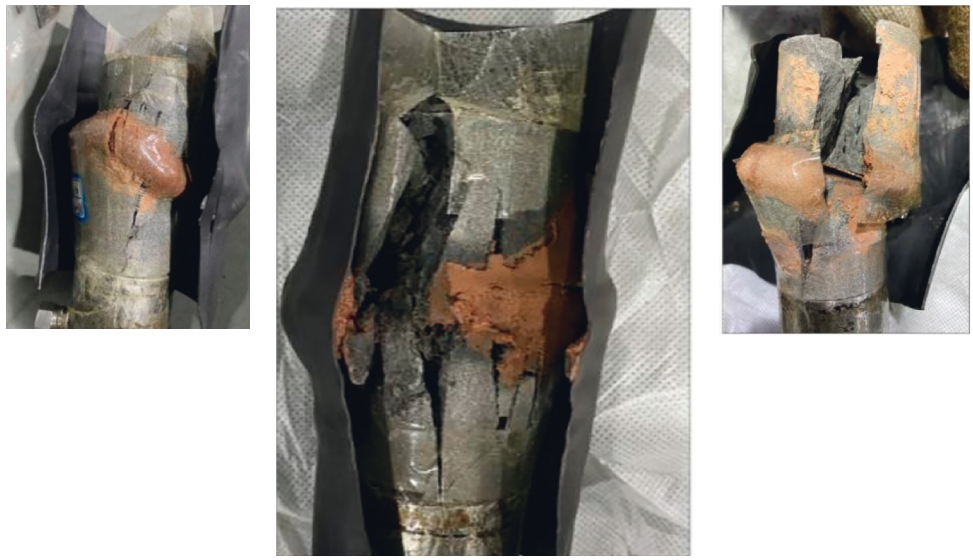

(a) (b) (c)

Figure 9: Slippage and macroscopic failure characteristics of joint plane with different roughness: (a) fine sandstone with fine sand, (b) fine sandstone with medium sand, and (c) fine sandstone with coarse sand.

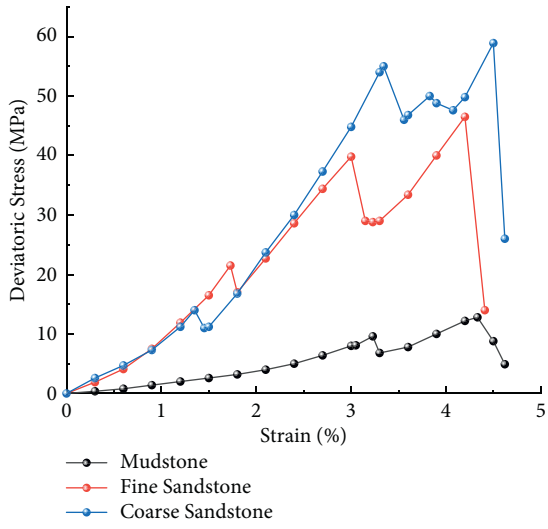

Figure 10: Stress evolution of specimens with different lithologies.

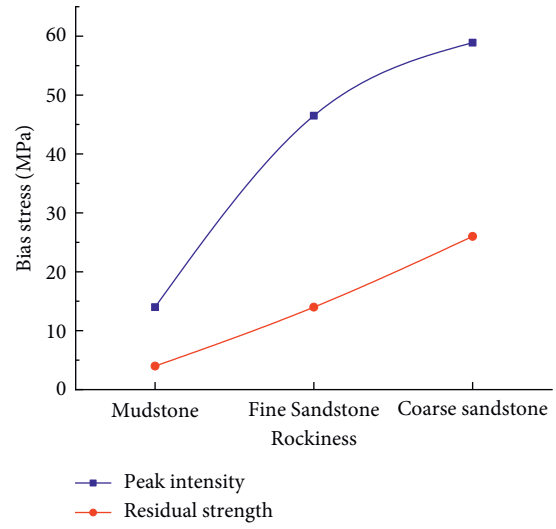

Figure 11: Variation curve of strength peak and residual strength of specimen with lithology.

Figure 9 shows the characteristics of joint plane slippage and macroscopic damage manifestation under different roughness. It can be seen that the smaller the roughness, the greater the dislocation and slip of the joint plane. As the roughness decreases, the splitting pattern develops from a single fracture to multiple fractures. Through careful observation of the specimen during the loading process, it is found that the duration of damage-crack propagation-

Table 3: Triaxial compression test of different lithology specimens.

Rockiness	Failure stress (MPa)		Elasticity modulus (GPa)
	σ_3	σ_1	
Mudstone	1	12.8	4.96
Fine sandstone	1	46.5	19
Coarse sandstone	1	58.9	22.4

(a) (b) (c)

Figure 12: Slippage and macroscopic failure characteristics of structural surfaces with different lithology specimens: (a) mudstone specimen, (b) fine sandstone specimen, and (c) coarse sandstone specimen.

splitting of the specimen with larger particle size on the structural surface is short, the splitting is completed almost instantaneously, the splitting crack is clear and obvious, and the sound is louder; for the specimen with smaller particle size, the crack propagates more slowly until the splitting, and the sound after splitting is small. During the loading process, for the test specimen with the coarse-grained structural surface, the particle in the filler experiences obvious crushing and shearing failure processes, and the bonding between the joint plane and the filler is good. As the loading continues, the joint plane stagger to a certain extent and stop sliding, and the specimen is split and damaged. As the particle size of the filler increases, the friction coefficient of the joint plane increases, and the friction force is increased after the sand is cemented with yellow mud through the process of pressing, shearing, and grinding. When the particle size of the filler is small, the friction coefficient is small, and the relative friction between the two disks is small, resulting in obvious dislocation.

3.3. Different Lithological (Strength) Stresses and Crack Evolution. The test results of the third scheme are shown in Figures 10 and 11. It can be seen that with the increase of the surrounding rock strength, the strain and the peak stress of the failed specimen increase continuously, the stress-strain curve gradually becomes steeper, and the accumulated energy before the movement of the joint plane gradually increases, which in turn increases the released energy during the activation of the joint plane. The peak strength and residual strength of the specimen both show an increasing trend with the increase of the surrounding rock strength, and the increased amplitude of the peak strength is much higher than that of the residual strength.

As shown in Figure 10 and Table 3, the elastic modulus of the specimen increases with the surrounding rock strength, and the stiffness of the coarse sandstone specimen is the largest.

Figure 12 shows the failure and slip characteristics of the specimens under different lithology conditions. It can be seen that the macroscopic fracture phenomena of the specimens with different lithologies are different. With the increase of the surrounding rock strength, the specimen developed from a small number of single splits to multiple split-penetrate failures. When the surrounding rock strength is low, a small sound is emitted when the specimen is damaged. With the increase of the surrounding rock strength, the intensity of the failure sound increases. When the coarse sandstone is damaged, a strong blasting sound is emitted, and part of the specimen collapses. For low-strength mudstone, cracks slowly generate, expand, and finally penetrate the specimen. The specimen has a better energy consumption effect during the loading failure

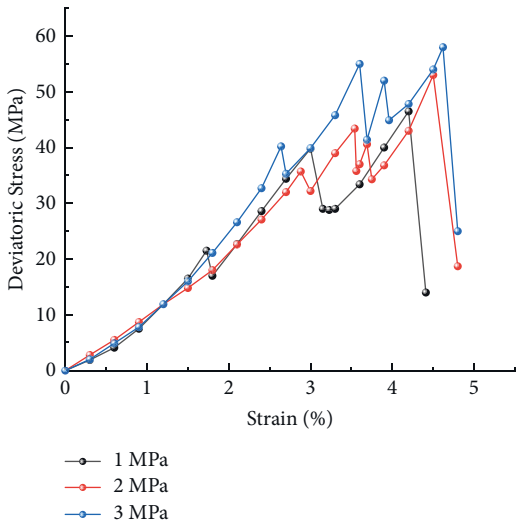

Figure 13: Stress-strain curves of fine sandstone specimens with different confining pressures.

process. For coarse sandstone with high strength, the development time from the fissures to the splitting is short, and a large amount of energy is released instantaneously. In actual production, the greater the strength of the surrounding rock, the greater the energy released and stored after the activation of the joint plane, which is more likely to induce dynamic disasters.

3.4. Stress and Crack Evolution under Different Confining Pressures. The test results of the fourth scheme are shown in Figure 13. It can be seen that with the increase of the confining pressure, the strength of the specimen also gradually increases. When the confining pressure is 1 MPa, the peak strength reaches 46.5 MPa; when the confining pressure is 2 MPa, the peak stress can reach 53.1 MPa, and when the confining pressure reaches 3 MPa, the peak stress is increased to 58.2 MPa. At the same time, the number of slips of the specimen increases significantly before reaching the ultimate strength, resulting in multiple slip-smoothing phenomena. It can be seen from Figure 14 that the increase in the confining pressure leads to a significant increase in the peak stress and residual strength of the specimen. When analyzing the residual strength of the specimen, it is found that the peak stress change curve and the residual strength change curve increase in the same way. Table 4 shows that the elastic modulus of the specimen increases slightly with the confining pressure, indicating that the confining pressure has little effect on the elastic modulus.

In order to further analyze the relationship between the confining pressure and the ultimate strength of the specimen, the confining pressure and the peak vertical stress of the specimen are linearly fitted as follows [25]:

$$\sigma_1 = m\sigma_3 + b, \quad (1)$$

where m and b are the slope and intercept of the fitting function, respectively, and the linear regression equation is shown in Figure 15.

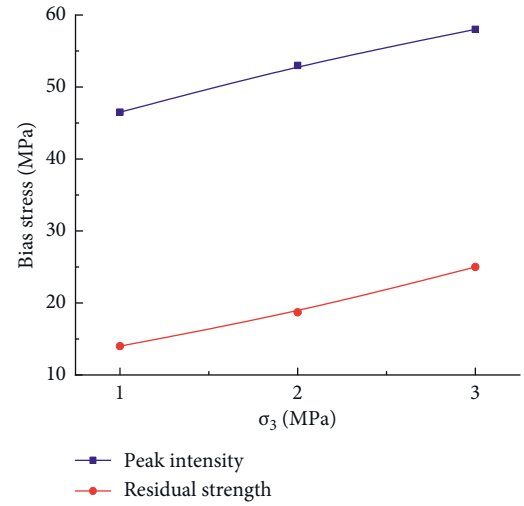

Figure 14: Variation curve of peak strength and residual strength of specimen with confining pressure.

Table 4: Triaxial compression test of fine sandstone specimens with different confining pressures.

Confining pressure σ_3 (MPa)	Failure stress σ_1 (MPa)	Elasticity modulus (GPa)
1	12.8	19
2	46.5	20.74
3	58.9	21.89

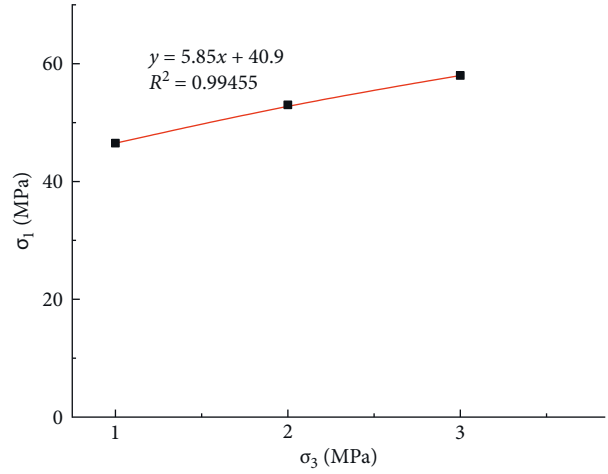

Figure 15: Linear regression of the relationship between ultimate strength of specimen and confining pressure.

It can be known that under the same joint plane angle, there is a linear relationship between the ultimate strength of the specimen and the confining pressure. The 0.99455 of R^2 reflects that the linear relationship is good. The regression coefficient is 5.85, and the intercept is 40.9. Within a certain range, with the increase of confining pressure, the strength of the fine sandstone specimen increases linearly. Figure 16 shows the fracture characteristics of fine sandstone specimens with a joint plane angle of 25° under different confining pressures. According to the analysis of the fracture

(a) (b) (c)

Figure 16: Fracture evolution characteristics of fine sandstone specimens under different confining pressures: (a) confining pressure 1 MPa, (b) confining pressure 2 MPa, and (c) confining pressure 3 MPa.

characteristics, the failure forms of mudstone are not exactly the same. At a lower confining pressure (Figures 16(a) and 16(b)), the specimen showed tensile fracture failure, and cracks with vertical bars perpendicular to the structural plane were generated and extended until penetration. When confining pressure is high, the failure mode of the specimen is *X* shear failure and fragmentation. At the same time, with the increase of confining pressure, the failure mode of the specimen changes from relatively complete to complete fracture.

The increase of confining pressure significantly improves the failure strength of the specimen and also leads to a significant increase in the number of cracks and the degree of failure when the specimen is damaged.

4. Conclusions

(1) The test results show that with the continuous increase of stress, the specimen occurred multiple slip-stabilization phenomena and experienced four stages during the loading process, including initial compaction, elastic deformation, brittle deformation, and residual strength, and the stress-strain curve presents wavy fluctuations.

(2) With the increase of the joint plane angle, the peak stress strength and residual strength of the specimens decrease significantly, and the macroscopic fracture damage characteristics of the rock gradually change from multiple cracks to a single crack, and the cracks were always perpendicular to the joint plane. Cracks always perpendicular to the joint plane show splitting damage, and when the joint plane angle is maximum, the specimen shows slip instability damage.

(3) The greater the roughness of the structural surface, the greater the peak stress and residual strength at the time of damage. Before the failure of the specimen, there are several obvious dislocations between the joint plane of the two disks, that is, the process of slip-stability-slip, the stress curve shows a wave-like change. As the roughness of the joint plane increases, the friction coefficient and the bearing stress of the specimen increase; the possibility of sliding on the joint plane decreases; and the damage mode develops from multiple fractures to single fractures.

(4) With the increase of the surrounding rock strength, the peak stress and residual strength of the specimen at the time of damage increase; the strain also increases; and the stress-strain curve gradually becomes steeper. With different lithologies, the macrofracture phenomenon of the damage process of the specimen is also different. With the increase of the surrounding rock strength, the specimen develops from single-strand splitting to multiple penetrating-splitting damage.

(5) With the increase of confining pressure, the peak stress and residual strength of the specimen at the time of damage increase significantly, and the number of slips of the specimen before reaching the ultimate strength increases significantly, resulting in multiple slip stability phenomenon, which also leads to the significant increase of the number of fractures and the degree of damage.

Data Availability

The data used to support the findings of this study are included within the article.

Conflicts of Interest

The authors declare that they have no conflicts of interest.

Acknowledgments

This research was supported by the discipline innovation team of Liaoning Technical University (LNTU20TD-05).

References

[1] S. Q. Yang, J. W. Lu, W. L. Tian, and J. Z. Tang, "Experimental study of mechanical behavior of rock specimens with different joint roughness coefficient under conventional triaxial compression," *Rock and Soil Mechanics*, vol. 39, no. S1, pp. 21–32, 2018.

[2] Z. D. Dong and H. Y. Tian, "Experimental study on the conventional triaxial compression of marble rock samples," *Soil Engineering and Foundation*, vol. 35, no. 5, pp. 635–639, 2021.

[3] M. H. Nasseri, K. S. Rao, and T. Ramamurthy, "Failure mechanism in schistose rocks," *International Journal of Rock Mechanics and Mining Sciences*, vol. 34, no. 3-4, pp. 219.e1–219.e15, 1997.

[4] H. Niandou, J. F. Shao, J. P. Henry, and D. Fourmaintraux, "Laboratory investigation of the mechanical behaviour of Tournemire shale," *International Journal of Rock Mechanics and Mining Sciences*, vol. 34, no. 1, pp. 3–16, 1997.

[5] H. J. Mao and C. H. Yang, "Study on effects of discontinuities on mechanical characters of slate," *Chinese Journal of Rock Mechanics and Engineering*, vol. 24, no. 20, pp. 3651–3656, 2005.

[6] J. X. Han, S. C Li, S. C Li, X. H. Tong, and W. T. Li, "Model study of strength and failure modes of rock mass with persistent cracks," *Rock and Soil Mechanics*, vol. 32, no. S2, pp. 178–184, 2011.

[7] J. L. Li, L. H. Wang, X. X. Wang, R. H. Wang, Z. Cheng, and D. Li, "Research on unloading nonlinear mechanical characteristics of jointed rock masses," *Journal of Rock Mechanics and Geotechnical Engineering*, vol. 2, no. 4, pp. 357–364, 2010.

[8] M. X. Liu, M. K. Liao, E. L. Liu, and Q. S. Zheng, "Experimental research on mechanical properties of jointed rock mass with different angles of angle," *Journal of Beijing University of Technology*, vol. 44, no. 03, pp. 336–343, 2018.

[9] Q. S. Zheng, E. L. Liu, and M. X. Liu, "Influence of the dip angle of joint planes on mechanical properties of artificial rock samples under triaxial test conditions," *Rock and Soil Mechanics*, vol. 40, no. 5, pp. 1854–1861, 2019.

[10] M. X. Liu and E. L. Liu, "Dynamic mechanical properties of artificial jointed rock samples subjected to cyclic triaxial loading," *International Journal of Rock Mechanics and Mining Sciences*, vol. 98, pp. 54–66, 2017.

[11] A. Mahboubi and A. Ajorloo, "Experimental study of the mechanical behavior of plastic concrete in triaxial compression," *Cement and Concrete Research*, vol. 35, no. 2, pp. 412–419, 2005.

[12] Y. Pashang Pisheh and S. M. Mir Mohammad Hosseini, "Stress-strain behavior of plastic concrete using monotonic triaxial compression tests," *Journal of Central South University*, vol. 19, no. 4, pp. 1125–1131, 2012.

[13] F. A. Donath, "Experimental study of shear failure in anisotropic rocks," *The Geological Society of America Bulletin*, vol. 72, no. 6, pp. 985–989, 1961.

[14] J. B. Walsh and W. F. Brace, "A fracture criterion for brittle anisotropic rock," *Journal of Geophysical Research*, vol. 69, no. 16, pp. 3449–3456, 1964.

[15] G. Reik and M. Zacas, "Strength and deformation characteristics of jointed media in true triaxial compression," *International Journal of Rock Mechanics and Mining Sciences & Geomechanics Abstracts& Geomechanics Abstracts*, vol. 15, no. 6, pp. 295–303, 1978.

[16] J. Q. He, Z. Li, Y. Liu, and W. H. Gao, "Numerical simulation of tri-axial compression test for rock mass with joint plane," *Mining and Metallurgical Engineering*, vol. 36, no. 4, pp. 1–4, 2016.

[17] T. Nishiyama, Y. Chen, H. Kusuda et al., "The examination of fracturing process subjected to triaxial compression test in Inada granite," *Engineering Geology*, vol. 66, no. 3-4, pp. 257–269, 2002.

[18] J. Arzúa, L. R. Alejano, and G. Walton, "Strength and dilation of jointed granite specimens in servo-controlled triaxial tests," *International Journal of Rock Mechanics and Mining Sciences*, vol. 69, pp. 93–104, 2014.

[19] R. Lagioia and R. Nova, "An experimental and theoretical study of the behaviour of a calcarenite in triaxial compression," *Géotechnique*, vol. 45, no. 4, pp. 633–648, 1995.

[20] S. Serdengecti and G. D. Boozer, "The effects of strain rate and temperature on the behavior of rocks subjected to triaxial compression: the 4th U.S," in *Proceedings of the Symposium on Rock Mechanics (USRMS)*, pp. 61–83, Oxford, UK, August, 1961.

[21] Q. B. Lin, P. Cao, S. Y. Mao, C. J. Ou, and R. H. Cao, "Fatigue behaviour and constitutive model of yellow sandstone containing pre-existing surface crack under uniaxial cyclic loading," *Theoretical and Applied Fracture Mechanics*, vol. 109, Article ID 102776, 2020.

[22] Y. Zhou, S. C. Wu, Y. T. Gao, and A. Misra, "Macro and meso analysis of jointed rock mass triaxial compression test by using equivalent rock mass (ERM) technique," *Journal of Central South University*, vol. 21, no. 3, pp. 1125–1135, 2014.

[23] M. Bahaaddini, G. Sharrock, and B. K. Hebblewhite, "Numerical investigation of the effect of joint geometrical parameters on the mechanical properties of a non-persistent jointed rock mass under uniaxial compression," *Computers and Geotechnics*, vol. 49, pp. 206–225, 2013.

[24] C. Lyu, J. Liu, Y. Ren, C. Liang, and Y Liao, "Study on very long-term creep tests and nonlinear creep-damage constitutive model of salt rock," *International Journal of Rock Mechanics and Mining Sciences*, vol. 146, Article ID 104873, 2021.

[25] C. Lyu, J. Liu, Y. Ren, C. Liang, and Y Zeng, "Mechanical characteristics and permeability evolution of salt rock under thermal-hydro-mechanical (THM) coupling condition," *Engineering Geology*, vol. 302, Article ID 106633, 2022.